Original Article

# Application of three-dimensional printed models with near-infrared fluorescence technology in video-assisted thoracoscopic surgery segmentectomy: a single-center propensity-score matching analysis

**Renjie Huang[1,2,3#], Jianting Du[1,3#], Guobing Xu[1,3], Xian Gong[1,3], Jiekun Qian[1,3], Shuxing Chen[2], Bin Zheng[1,3], Chun Chen[1,3*], Zhang Yang[1,3*]**

[1]Department of Thoracic Surgery, Fujian Medical University Union Hospital, Fuzhou, China; [2]Department of Thoracic Surgery, Fuzhou Pulmonary Hospital of Fujian, Fuzhou, China; [3]Key Laboratory of Cardio-Thoracic Surgery, Fujian Medical University, Fuzhou, China

*Contributions:* (I) Conception and design: R Huang, J Du; (II) Administrative support: B Zheng, S Chen, C Chen; (III) Provision of study materials or patients: R Huang, S Chen; (IV) Collection and assembly of data: R Huang, J Du; (V) Data analysis and interpretation: R Huang, B Zheng, Z Yang, C Chen; (VI) Manuscript writing: All authors; (VII) Final approval of manuscript: All authors.

[#]These authors contributed equally to this work as co-first authors.

[*]These authors contributed equally to this work.

*Correspondence to:* Zhang Yang, MD, PhD; Chun Chen, MD. Department of Thoracic Surgery, Fujian Medical University Union Hospital, No. 29, Xinquan Road, Fuzhou 350000, China; Key Laboratory of Cardio-Thoracic Surgery, Fujian Medical University, Fuzhou, China.
Email: fjxh_zhang2021@163.com; chenchun0209@fjmu.edu.cn.

**Background:** The combination of three-dimensional printing (3DP) technology and near-infrared fluorescence (NIF) technology using indocyanine green (ICG) has demonstrated significant potential in enhancing surgical margin and safety, as well as simplifying segmental resection. However, there is limited literature available on the integrated use of these techniques. The current study assessed the effectiveness and value of integrating 3DP-NIF technologies in the perioperative outcomes of thoracoscopic segmental lung resection.

**Methods:** This single-center, retrospective study recruited 165 patients with pulmonary nodules who underwent thoracoscopic segmentectomy. Eligible patients were categorized into two groups: the 3DP-NIF group (71 patients) treated with a combination of 3DP-NIF technology, and the three-dimensional computed tomography bronchography and angiography with modified inflation-deflation (3D-CTBA-ID) group (94 patients). Following rigorous propensity-score matching (PSM) analysis (1:1 ratio), perioperative outcomes between these two approaches were compared.

**Results:** Sixty-six patients were successfully matched in each group. In the 3D-CTBA-ID group, inadequate visualization of segmental planes was noted in 14 cases, compared to only five cases in the 3DP-NIF group (P=0.03). In addition, the 3DP-NIF group demonstrated a shorter time for clear intersegmental boundary line (IBL) presentation {9 [8, 10] *vs.* 1,860 [1,380, 1,920] s} (P<0.001), and shorter operative time (134.09±34.9 *vs.* 163.47±49.4 min) (P<0.001), postoperative drainage time (P<0.001), and postoperative hospital stay (P=0.002) compared to the 3D-CTBA-ID group. Furthermore, the incidence of postoperative air leak was higher in the 3D-CTBA-ID group than in the 3DP-NIF group (33.3% *vs.* 7.6%, P<0.001).

**Conclusions:** The combination of 3DP-NIF technologies served as a reliable technical safeguard, ensuring the safe and efficient execution of thoracoscopic pulmonary segmentectomy.

**Keywords:** Three-dimensional printing (3DP); near-infrared fluorescence imaging (NIF imaging); propensity-score matching (PSM); segmentectomy; lung cancer

Submitted Mar 25, 2024. Accepted for publication Jun 07, 2024. Published online Jul 26, 2024.
doi: 10.21037/jtd-24-489
**View this article at:** https://dx.doi.org/10.21037/jtd-24-489

## Introduction

As well documented, lung cancer is a prevalent malignancy characterized by significantly high incidence and high mortality rates globally (1). Recent advances in medical imaging, encompassing the utilization of artificial intelligence (AI) and low-dose computed tomography (CT), have substantially optimized the detection of small peripheral lung nodules with the potential to progress to non-small cell lung cancer (NSCLC) (2,3). A meta-analysis study reported that the difference in disease-free survival (DFS) or overall survival (OS) for stage I NSCLC patients who underwent segmental lung resection compared to those who underwent lobectomy was not statistically significant (4), suggesting that segmental lung resection could be a viable alternative to lobectomy, particularly in cases where lobectomy might not be an option due to poor lung function or other comorbidities.

The challenges associated with segmental resection exceed that of lobectomy, attributable to frequent anatomical variations in lung segments, notably within the vascular and bronchial systems (5). The advent of three-dimensional computed tomography bronchography and angiography (3D-CTBA) or three-dimensional (3D) printed models has been instrumental in enhancing the understanding of precise anatomical relationships within pulmonary structures. This advancement has enabled greater precision and accuracy during surgical interventions, thus leading to improved patient outcomes (6). In comparison to 3D reconstructed virtual images, 3D printed models offer surgeons a more tangible representation conducive to the identification of complex entangled blood vessels and bronchial tubes prior to surgery (7).

Accurate identification of intersegmental planes in anatomical lung segment resection is crucial. Currently, two primary methods are extensively employed: the modified inflation-deflation (ID) method (8) and near-infrared fluorescence (NIF) technology combined with intravenous injection of indocyanine green (ICG) (9). Earlier studies have confirmed that the intersegmental intervals observed through the NIF method exhibit a high level of consistency with those noted by the ID method, accurately reflecting the actual intersegmental intervals. The NIF strategy displays several benefits over the ID approach in chronic obstructive pulmonary disease (COPD) or emphysema patients, including minimal disruption of the surgical field, shorter surgery duration, and faster identification of intersegmental connections (10,11).

The present study aimed to assess the effectiveness and value of a combined approach integrating 3D printed models and NIF technology on perioperative outcomes following thoracoscopic segmental lung resection. Perioperative outcomes of patients who underwent this procedure were evaluated using propensity-score matching (PSM) analysis to mitigate the risk of selection bias in this retrospective study. We present this article in accordance with the STROBE reporting checklist (available at https://jtd.amegroups.com/article/view/10.21037/jtd-24-489/rc).

### Highlight box

**Key findings**

- The combination of three-dimensional printing (3DP) technology and near-infrared fluorescence (NIF) (3DP-NIF) technology is highly valuable for improving surgical resection rates and safety as well as simplifying segmental resection.

**What is known and what is new?**

- Challenges may be encountered in interpreting 3D virtual reconstruction images on a two-dimensional screen, particularly during complicated lung segmental surgeries; chronic obstructive pulmonary disease or emphysema patients, the modified inflation-deflation (ID) method commonly used to identify the intersegmental plane may result in inaccurate resection due to prolonged visualization time.
- Perioperative outcomes between 3DP-NIF technology and three-dimensional computed tomography bronchography and angiography with modified ID technology were compared.

**What is the implication, and what should change now?**

- The combination of 3DP technology and NIF technology served as a reliable technical safeguard, ensuring the safe and efficient execution of thoracoscopic pulmonary segmentectomy.

## Methods

### *Study design*

This retrospective study was conducted at Fuzhou Pulmonary Hospital (Fujian, China) between January 2020 and April 2023, enrolling 165 patients with pulmonary nodules who underwent thoracoscopic segmentectomy employing different combinations of techniques (*Table 1*). After PSM, 66 cases were assigned to the 3DP-NIF group, while 66 cases belonged to the 3D-CTBA-ID group. The study was designed to evaluate the effectiveness and value of the combination of 3DP-NIF in video-assisted thoracoscopic surgery (VATS) segmentectomy. The flow diagram of the study is illustrated in *Figure 1*. The study was

**Table 1** Clinical characteristics of NSCLC patients

| Characteristics | Before PSM | | | After PSM | | |
|---|---|---|---|---|---|---|
| | 3DP-NIF group (n=71) | 3D-CTBA-ID group (n=94) | P value | 3DP-NIF group (n=66) | 3D-CTBA-ID group (n=66) | P value |
| Sex | | | 0.29 | | | 0.69 |
| Male | 18 (25.4) | 31 (33.0) | | 18 (27.3) | 16 (24.2) | |
| Female | 53 (74.6) | 63 (67.0) | | 48 (72.7) | 50 (75.8) | |
| Age (years) | 53.14±11.18 | 54.39±11.47 | 0.48 | 53.58±11.2 | 53.32±11.19 | 0.90 |
| BMI (kg/m$^2$) | 23.34 [21.09, 25.46] | 22.34 [21.09, 24.78] | 0.43 | 23.24 [21.09, 25.47] | 22.58 [21.2, 25.07] | 0.96 |
| $FEV_1$ (L) | 2.23 [1.96, 2.50] | 2.12 [1.9, 2.34] | 0.30 | 2.22 [1.95, 2.47] | 2.15 [1.93, 2.60] | 0.86 |
| Smoking history | | | 0.62 | | | 0.39 |
| Yes | 19 (26.8) | 22 (23.4) | | 16 (24.2) | 12 (18.2) | |
| No | 52 (73.2) | 72 (76.6) | | 50 (75.8) | 54 (81.8) | |
| COPD | | | 0.73 | | | >0.99 |
| Yes | 12 (16.9) | 14 (14.9) | | 12 (18.2) | 12 (18.2) | |
| No | 59 (83.1) | 80 (85.1) | | 54 (81.8) | 54 (81.8) | |
| Tumor size (mm) | 9 [7, 12] | 10 [8, 12] | 0.18 | 9 [7, 12] | 9 [7.75, 11.25] | 0.65 |
| Type of segmentectomy | | | 0.09 | | | 0.38 |
| Simple segmentectomy | 9 (12.7) | 5 (5.3) | | 8 (12.1) | 5 (7.6) | |
| Complex segmentectomy | 62 (87.3) | 89 (94.7) | | 58 (87.9) | 61 (92.4) | |

Data are presented as n (%), mean ± SD or median [P25, P75]. NSCLC, non-small cell lung cancer; PSM, propensity-score matching; 3DP, three-dimensional printing; NIF, near-infrared fluorescence; 3D-CTBA, three-dimensional computed tomography bronchography and angiography; ID, inflation-deflation; BMI, body mass index; $FEV_1$, forced expiratory volume in one second; COPD, chronic obstructive pulmonary disease; SD, standard deviation.

conducted in accordance with the Declaration of Helsinki (as revised in 2013). The study was approved by the Medical Ethics Committee of Fuzhou Pulmonary Hospital, Fuzhou, Fujian Province, China (approval No. 2024004-01) and informed consent was obtained from all individual participants.

### *Patient selection*

Eligibility criteria were as follows: (I) clinical diagnosis of early-stage NSCLC with a tumor diameter of ≤2 cm; (II) thoracoscopic segmentectomy performed in accordance with the National Comprehensive Cancer Network (NCCN) guidelines for NSCLC (12) and the design of this study; (III) no age or gender restrictions; (IV) routine cardiopulmonary function assessment to determine eligibility for surgery and absence of distant metastases; (V) no prior neoadjuvant chemotherapy or radiotherapy treatment.

The exclusion criteria for segmentectomy in this retrospective study were as follows: (I) a history of allergy to iodine or ICG; (II) pulmonary nodules that can be excised by pulmonary wedge resection and primary tumors requiring lobectomy; (III) surgical unfitness.

### *Preoperative 3D-CTBA reconstruction and 3D model printing*

A high-speed 64-channel multi-detector CT scanner (SOMATOM Definition AS, Siemens, Germany) with 1.2-mm pitch and 1.0-mm scanning thickness was employed in this study. All patients underwent CT scans and 3D-CTBA for tumor localization, anatomical relationships and variations determination, and surgical procedure simulation.

Digital Imaging and Communications in Medicine (DICOM) data from thin-slice (0.625–1.25 mm) CT images

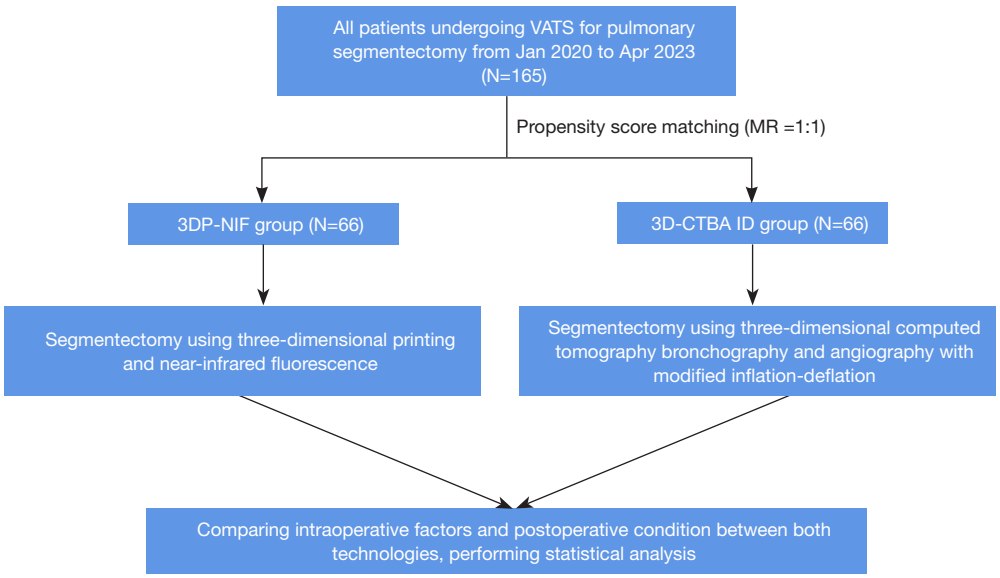


**Figure 1** The flow diagram of the study. VATS, video-assisted thoracic surgery; MR, match ratio; 3DP, three-dimensional printing; NIF, near-infrared fluorescence; 3D-CTBA-ID, three-dimensional computed tomography bronchography and angiography with modified inflation-deflation.

were imported into Wedge Medical Image Processing Software (developed by Ningbo Wedge Medical Technology Co., Ltd.) for 3D reconstruction of bronchial and vascular vessels. Threshold segmentation combined with the regional growth method was adopted for rapid planar segmentation, ensuring the shortest distance from the resection edge of the lung parenchyma to the edge of the tumor was greater than 2 cm or the maximum size of the tumor.

For the 3D printed model set, the "stereolithography (STL)" file format generated from the reconstructed images was exported and saved. The STL format file of the 3D digital model was used to set the printing parameters, such as layer thickness, printing speed, and fill density, as per the printer specifications. The YDM-1LC-295165 printer (developed by Shenzhen Yidimu Intelligent Technology Co., Ltd., Shenzhen, China) was used for printing, with photosensitive resin as consumable (Shenzhen Yidimu Intelligent Technology Co., Ltd.). Ultimately, arteries, veins, tracheobronchial trees, and the 3D lung model prototypes were generated.

### *Surgical procedures*

All surgical procedures were conducted by the same surgical team of five chief physicians, each possessing a minimum of 10 years of experience in thoracoscopic surgery. Prior to segmental lung surgery, the lung nodules were precisely localized using 3D reconstruction or 3D printed lung models. The surgical procedure was meticulously planned to ensure adequate surgical margins. An in-depth analysis and confirmation of the arteries, veins, and bronchi of the target segments was conducted. General anesthesia was administered to all patients, along with double-lumen tracheal intubation and one-lung ventilation. A two- or three-port approach for thoracoscopic lung segmental surgery was selected based on the discretion of the surgeon. The conventional thoracoscopic equipment utilized in this study was the KARL STORZ thoracoscopic system from Germany, whilst the fluorescent thoracoscopic equipment was domestic OptoMedic (model OPTA-CAM2, Guangdong, China).

During the surgical intervention, the target arteriovenous and bronchial segments were identified based on 3D-CTBA or 3D printed lung models (*Figures 2,3*). In the 3D-CTBA-ID group, the 3D-CTBA data were transferred to a computer and presented to the other surgeons in the operating room. Conversely, a personalized 3D printed model was positioned in front of the thoracoscopic screen in the 3DP group, allowing real-time navigation through the model and verification of segmental vessel and bronchial tube morphology. Intraoperative lymph node sampling was routinely performed and submitted for intraoperative frozen

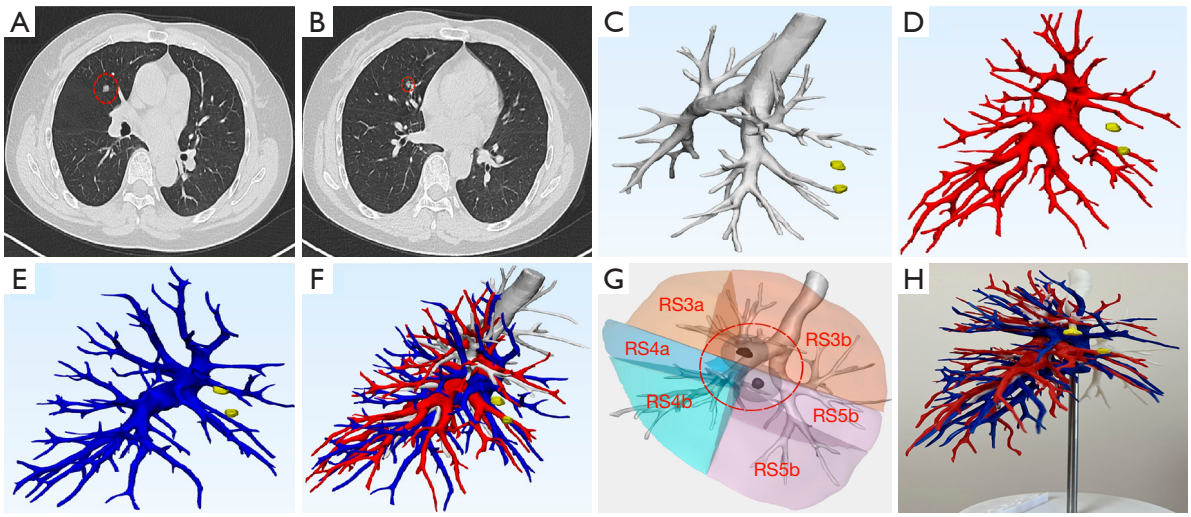


**Figure 2** A case of personalized preoperative planning process using 3D-CTBA and 3D printing model. (A,B) The patient's CT showing two mGGN in right lung; red dotted circles indicate the location of the lung nodules. (C-F) The patient's 3D-CTBA reconstruction, including lung bronchus, arteries and veins. (G) The location of the two nodules and the target segments of the lung to be resected; red dotted circles indicate the location of the lung nodules. (H) The patient's 3D printing model provides visualization of the location of the lesion and the anatomy of the target area. 3D-CTBA, three-dimensional computed tomography bronchography and angiography; CT, computed tomography; mGGN, mixed ground-glass nodule.

pathological examination. The intersegmental planes were identified using either the ID method or NIF technology.

The NIF technology combined with the intravenous injection of ICG involved the administration of a bolus comprising 2 mL ICG (25 mg dissolved in 10 mL saline, equivalent to 5 mg/body weight) into the peripheral vein using the NIF thoracoscopic fluorescence mode. After 7–15 s, the target segment to be resected remained uncolored. In contrast, the remaining lung tissues were highlighted in green (*Figure 3*), allowing clear demarcation of intersegmental boundaries on the pleural surface.

The modified ID method consisted of cutting the artery and bronchus of the target segment. The anaesthesiologist subsequently inflated the lung on the operated side with pure oxygen before switching to one-lung ventilation on the healthy side. This procedure resulted in the target segment remaining inflated for approximately 15 min while the rest of the lung tissues atrophied. The inter-segmental boundary between the expanded and atrophied areas on the pleural surface was evident (*Figure 3*).

Surgical margins for all malignant nodules were maintained at ≥2 cm or larger than the tumor diameter. Intersegmental surfaces were marked using an electrocoagulation hook or argon knife jet coagulation in both groups. Target lung segments were dissected using an energy device combined with a thoracoscopic linear cutting anastomosis technique. Complete lobectomy was performed in cases of lymph node metastases or insufficient surgical margins.

Pulmonary segmentectomies were classified as either simple or complex. The former included the upper segment of the right or left lower lobe (segment 6), the upper left intrinsic segment ($LS^{1+2+3}$), and the upper left lingual segment ($LS^{4+5}$), whereas the latter encompassed the remaining lung segments in addition to the simple segmental resection.

### *Observational indicators*

This present study primarily collected general and perioperative data from the two groups. Perioperative data encompassed operation time, clarity of target lung segment display (including clear display time and cases with unclear display), intraoperative blood loss volume, frequency of conversion to thoracotomy, number of mediastinal lymph node sampling/dissection procedures, duration of the indwelling postoperative drainage tube, length of postoperative hospital stay, postoperative pathological conditions, and early postoperative complications (such as pulmonary infection and pulmonary air leakage), among

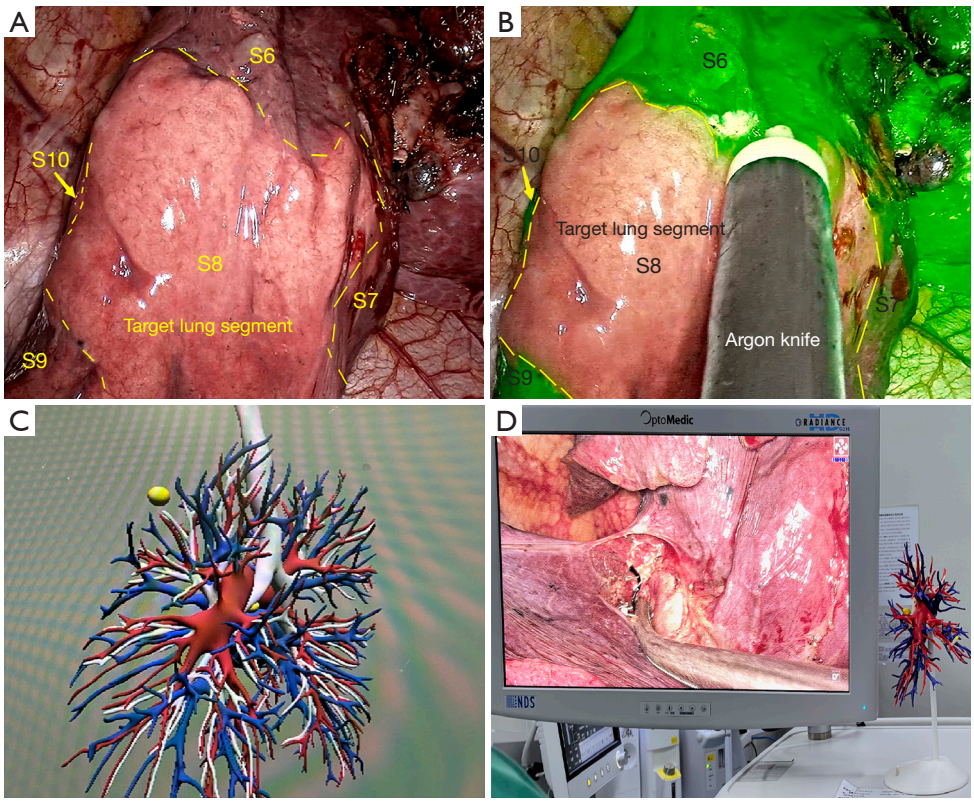


**Figure 3** Different methods to visualize target lung segments. (A) Modified inflation-deflation method to reveal target lung segments. Reprinted with permission from (13). (B) NIF technology fluorescence pattern reveals target lung segments. Reprinted with permission from (13). (C) 3D-CTBA-ID reconstruction on a 2D screen. (D) A 3D printed model combined with near-infrared fluorescent thoracoscopy for lung segment surgery. Reprinted with permission from (13). NIF, near-infrared fluorescence; 3D-CTBA-ID, three-dimensional computed tomography bronchography and angiography with modified inflation-deflation; 2D, two-dimensional.

other relevant indicators.

The duration of the operation was defined as the time from the initiation of the skin incision to the completion of the skin suture. Notably, the methods for timing the display of the target lung segment differed. The ICG fluorescence method involved injecting ICG from a peripheral vein into the target lung segment, resulting in a color contrast with the rest of the lung tissue. In the modified ID method, the lung tissue was expanded from the beginning of lung tissue inflation until the target lung segment was still in an inflated state; the remaining lung tissue appeared to be completely deflated, forming a clear ID junction line.

### *Statistical analysis*

SPSS 27.0 for Windows (IBM, Armonk, NY, USA) was used for statistical analyses. PSM was used to minimize the impact of potential confounders and selection bias in baseline patient characteristics, including gender, age, body mass index (BMI), forced expiratory volume in one second ($FEV_1$), smoking history, COPD, tumor size, and type of segmentectomy. Following 1:1 PSM, the perioperative outcomes of both approaches were compared.

Continuous data conforming to normal distribution were expressed as mean ± standard deviation and analyzed using the *t*-test for independent data. Non-normally distributed data were expressed as median (P25, P75), with comparisons between groups performed using the Mann-Whitney *U*-test. Count data were denoted as number (n) and percentage (%) and compared using the $\chi^2$ test or Fisher's exact probability method. All tests were two-sided, with P values <0.05 deemed statistically significant.

**Table 2** Intraoperative and postoperative data

| Variables | 3DP-NIF group (n=66) | 3D-CTBA-ID group (n=66) | P value |
|---|---|---|---|
| Operation time (min) | 134.09±34.9 | 163.47±49.4 | <0.001 |
| Presentation time (s) | 9 [8, 10] | 1,860 [1,380, 1,920] | <0.001 |
| Not clear intersegmental plane | 5 (7.6) | 14 (21.2) | 0.03 |
| Blood loss (mL) | 20 [20, 30] | 20.00 [18.75, 30] | 0.68 |
| Number of lymph node resection | 4 [3, 5] | 4 [3, 5] | 0.20 |
| Drainage duration (days) | 2.00 [2, 2] | 2.00 [2, 3] | <0.001 |
| Hospital stays after surgery (days) | 5.00 [4.75, 6] | 6 [5, 7] | 0.002 |
| Postoperative early complications | | | |
| Pulmonary infection | | | 0.27 |
| No | 64 (97.0) | 60 (90.9) | |
| Yes | 2 (3.0) | 6 (9.1) | |
| Postoperative air leak ≥1 day | | | <0.001 |
| No | 61 (92.4) | 44 (66.7) | |
| Yes | 5 (7.6) | 22 (33.3) | |

Data are presented as n (%), mean ± SD or median [P25, P75]. 3DP, three-dimensional printing; NIF, near-infrared fluorescence; 3D-CTBA, three-dimensional computed tomography bronchography and angiography; ID, inflation-deflation; SD, standard deviation.

## Results

### *Clinical characteristics of the patients*

Data collected from January 2020 to April 2023 involved 165 patients with pulmonary nodules who underwent thoracoscopic segmentectomy. The clinical characteristics of the patients, divided into two groups, are summarized in *Table 1*. The 3DP-NIF group, consisting of 71 patients, underwent thoracoscopic segmentectomy using a combination of 3D printed models and NIF technology. Meanwhile, the 3D-CTBA-ID group, comprising 94 patients, underwent thoracoscopic segmentectomy using 3D computed tomography bronchial angiography and modified ID techniques. Prior to PSM, no statistical differences were noted between the two groups in terms of gender, age, BMI, $FEV_1$, smoking history, COPD, tumor size, and type of segmentectomy (*Table 1*). Post-PSM, 66 patients in each group were successfully matched.

### *Intraoperative and postoperative data*

All segmentectomies in each group were performed without conversion to thoracotomy. Frozen section analysis of lymph nodes yielded negative results in all cases; thus, lobectomy was not performed. Intraoperative findings indicated that vascular-bronchial branches identified through 3D-CTBA and the 3D printed models corresponded with the actual pulmonary vascular-bronchial branches. Moreover, aberrant bronchi and blood vessels were accurately identified by either 3D-CTBA or 3D printed models. Following the application of these technologies, both groups achieved sufficient oncological margin length to meet the requirements of surgical quality control. None of the 66 patients in the 3D-NIF group experienced adverse reactions subsequent to ICG administration.

Intraoperative and postoperative data, such as presentation time, blood loss, number of lymph node resections, drainage duration, postoperative hospital stay, and early postoperative complications (including pulmonary infection and postoperative air leak time), did not follow a normal distribution; therefore, the results were expressed in median (P25, P75) range. Comparisons between the two groups were conducted using the Mann-Whitney *U*-test. The results are presented in *Table 2*.

The data, as detailed in *Table 1*, revealed no statistical difference in the proportion of complex segmental resections between the 3DP-NIF group (87.9%) and the 3D-CTBA-ID group (92.4%) (P=0.38). Detailed

**Table 3** Segmentectomy position and number of cases

| Position | 3DP-NIF group (n=66) | 3D-CTBA-ID group (n=66) |
|---|---|---|
| Simple segmentectomy | | |
| Right lobe | | |
| $RS^{6}$ | 2 (3.0) | 2 (3.0) |
| Left lobe | | |
| $LS^{1+2+3}$ | 2 (3.0) | – |
| $LS^{4+5}$ | 2 (3.0) | 1 (1.5) |
| $LS^{6}$ | 2 (3.0) | 2 (3.0) |
| Complex segmentectomy | | |
| Right lobe | | |
| $RS^{1}$ | 7 (10.6) | 13 (19.7) |
| $RS^{1}a$ | 2 (3.0) | 1 (1.5) |
| $RS^{1}b$ | – | 1 (1.5) |
| $RS^{1}a + RS^{2}a$ | 1 (1.5) | – |
| $RS^{1} + RS^{2}$ | 5 (7.6) | 1 (1.5) |
| $RS^{2}$ | 6 (9.1) | 6 (9.1) |
| $RS^{2} + RS^{1}a$ | 1 (1.5) | – |
| $RS^{2}b$ | 1 (1.5) | – |
| $RS^{2}b + RS^{3}a$ | 2 (3.0) | 1 (1.5) |
| $RS^{3}$ | 3 (4.5) | 6 (9.1) |
| $RS^{3} + RS^{1}b$ | – | 1 (1.5) |
| $RS^{7} + RS^{8}$ | 1 (1.5) | 1 (1.5) |
| $RS^{8}$ | 4 (6.1) | 3 (4.5) |
| $RS^{8}a$ | 1 (1.5) | – |
| $RS^{8} + RS^{9}$ | 1 (1.5) | 2 (3.0) |
| $RS^{9}$ | 1 (1.5) | 1 (1.5) |
| $RS^{9} + RS^{10}$ | – | 1 (1.5) |
| $RS^{9} + RS^{10}b$ | – | 1 (1.5) |
| $RS^{10}$ | – | 1 (1.5) |
| $RS^{10}a$ | 1 (1.5) | – |
| $RS^{10}c$ | – | 1 (1.5) |
| Left lobe | | |
| $LS^{1+2}$ | 6 (9.1) | 6 (9.1) |
| $LS^{1+2}a$ | 1 (1.5) | 1 (1.5) |
| $LS^{1+2}c$ | 1 (1.5) | 1 (1.5) |
| $LS^{1+2}(a+b)$ | – | 2 (3.0) |
| $LS^{1+2}(b+c)$ | 1 (1.5) | – |
| $LS^{1+2}a + LS^{3}c$ | – | 1 (1.5) |
| $LS^{1+2}(a+b) + LS^{3}c$ | – | 1 (1.5) |
| $LS^{3}$ | 6 (9.1) | 1 (1.5) |
| $LS^{3}c$ | – | 1 (1.5) |
| $LS^{3}(b+c)$ | 2 (3.0) | – |
| $LS^{6}b + LS^{9}a$ | – | 1 (1.5) |
| $LS^{8}$ | 3 (4.5) | 2 (3.0) |
| $LS^{7+8}$ | 1 (1.5) | – |
| $LS^{7+8} + S^{10}b$ | – | 1 (1.5) |
| $LS^{9}$ | – | 2 (3.0) |

Data are presented as n (%). 3DP, three-dimensional printing; NIF, near-infrared fluorescence; 3D-CTBA, three-dimensional computed tomography bronchography and angiography; ID, inflation-deflation; RS, right segments; LS, left segments.

information regarding accurate nodule location and segmentectomy position is presented in *Table 3*. Notably, the 3DP-NIF group demonstrated a significantly shorter time for clear presentation of the intersegmental boundary line (IBL) {9 [8, 10] *vs.* 1,860 [1,380, 1,920] s} (P<0.001), a shorter operative time (134.09±34.9 *vs.* 163.47±49.4 min) (P<0.001), a reduced postoperative drainage time (P<0.001), and a shorter postoperative hospital stay (P=0.002) compared to the 3D-CTBA-ID group. In the 3D-CTBA-ID group, 14 cases exhibited unclear visualization of the intersegmental plane. Of note, prolonged waiting time did not reveal a distinct boundary in these cases, which included five $RS^{1}$ resections, two $RS^{2}$ resections, one $RS^{3}$ resection, one $RS^{8+9}$ resection, one $RS^{9+10}b$ resection, one

$RS^{10}$c resection, two $LS^{1+2}$ resections, and one $LS^{1+2}$(a+b) resection. Although most cases in the 3DP-NIF group demonstrated superior visualization of intersegmental planes, unclear delineation was noted in five cases: one $RS^{1}$ resection, one $RS^{1+2}$ resection, one $RS^{8}$a resection, and two involving $LS^{1+2}$(b+c) and $LS^{3}$ resections (P=0.03). Importantly, the incidence of postoperative air leaks was higher in the 3D-CTBA-ID group (33.3% *vs.* 7.6%, P<0.001). With the exception of COPD, the frequency of other comorbidities and complications was insufficient to allow for statistical comparison. No statistical differences were observed between the groups in terms of intraoperative blood loss volume (P=0.68), the incidence of postoperative pulmonary infection (P=0.27), and the number of lymph node dissection (P=0.20).

## Discussion

NSCLC can be efficiently treated through minimally invasive surgical modalities, particularly when diagnosed in the early stages (14). Since the 1990s, thoracic surgeons have widely adopted lobectomy and systemic lymph node dissection as the gold standard for the treatment of patients with completely resectable clinical stage I NSCLC (15). With the popularization of precision surgery and the continuous advancement of surgical strategies, lung segmental resection techniques have garnered significant attention, resulting in widespread application in clinical practice. Previous research indicated that segmental resection is a non-inferior alternative to lobectomy in the long term for patients with small nodules (below 2 cm), with the added benefit of superior lung function preservation while ensuring efficient lesion removal (16-18). In the current study, both patient groups were in optimal health with adequate lung function prior to surgery since the majority of minor ground-glass opacity (GGO) lesions were detected during routine physical examinations.

Segmental resection is more technically demanding and challenging compared to wedge resection and lobectomy. Successful anatomical segmental lung resection necessitates several crucial factors: (I) accurate localization of the lesion; (II) identification of the anatomical structures within the target lung segment; (III) techniques for identifying and isolating the target segments of the lung.

Precise localization of lung nodules is critical for successful surgery execution. Historically, superficial nodules are localized using methods such as finger palpation, CT-guided hook-wire localization, and fluorescence techniques (19,20). However, for deeper nodules requiring anatomical segmental lung resection, finger palpation or hook-wire localization is ineffective for accurate localization. Building upon previous research (21,22) and the insights from the present study, we posit that preoperative 3D reconstruction or 3D printed models can assist in identifying specific lung segments containing lesions. This approach could not only enable targeted lung segment resection but also streamline the lesion localization and excision processes, consequently diminishing the financial burden and psychological stress associated with invasive preoperative localization techniques.

The anatomical structure of lung segments and surgical operations are relatively complex. Variations in lung segment anatomy among patients complicate the accurate identification of arteries, veins, and bronchi within the target area. Therefore, accurate preoperative planning is crucial for thoracoscopic procedures to mitigate risks and postoperative complications (23). 3D-CTBA reconstruction is widely recognized as a valuable technique for anatomical lung segmental resection surgery. However, challenges may be encountered in interpreting 3D virtual reconstruction images on a 2D screen, particularly during complicated lung segmental surgeries, without a more user-friendly model for reference. In this study, either 3D-CTBA or 3D printed models were utilized for preoperative analysis, providing detailed anatomical representations of lung segments in the target area consistent with actual anatomical structures observed during the intervention. Additionally, vessels with variants could be identified in advance, thus lowering the likelihood of intraoperative injury. Preoperative 3D reconstruction or 3D printed models reduced vessel injury-related intraoperative bleeding in both groups of patients, with no statistical difference observed in intraoperative bleeding volumes between the two groups (P=0.68). Compared to 3D-CTBA, 3D printed models offer several advantages: (I) visual analysis of personalized 3D printed models, the planning of surgical processes, the simulation of the surgical steps, and the formulation of a robust resection strategy by surgeons; (II) enhanced visualization of blood vessel distribution within the target area by positioning the 3D printed model in front of the display for real-time intraoperative navigation; (III) expediting the understanding of lung segment anatomical structures among young surgeons through the use of 3D printed models, thereby reducing the learning curve (24).

In precise anatomical lung segmental resection, the

accurate identification of the intersegmental plane of the lung segment is crucial, directly impacting compliance with surgical margin distances and the incidence of postoperative complications. However, in COPD patients with extensive pleural adhesions, the modified ID method commonly used to identify the intersegmental plane may result in inaccurate resection due to prolonged visualization time (25). Recently, an increase in the utilization of the ICG fluorescence technique for assessing the intersegmental plane of lung segments has been observed (26). No adverse events were recorded in the present study following the intravenous administration of low-dose ICG (0.25 mg/kg) and a subsequent second dose for intraoperative needs, consistent with previous findings that an intravenous ICG dose ranging from 3.0 to 5.0 mg/kg is safe and well-tolerated (27,28). The 3DP-NIF group exhibited a significantly shorter time for clear presentation of the IBL compared to the 3D-CTBA-ID group {9 [8, 10] *vs.* 1,860 [1,380, 1,920] s} (P<0.001), thereby implying that the clarity in fluorescence imaging was contingent upon both ICG concentration and arterial blood flow distribution within target lung segments. Therefore, this technique may be more appropriate than the modified ID method for VATS segmental lung resection in patients with comorbid chronic lung disease or a history of long-term smoking. Furthermore, the intersegmental plane rendering through fluorescence imaging relies on the accuracy of arterial dissections within target lung segments. Excessive arterial dissections might result in increased loss of lung tissue, whilst fewer dissections could increase susceptibility to air leaks, a common complication following elective lung resection (29). Surprisingly, complex segmental resections were more prevalent than simple segmental resections in both groups, with *Tables 1*,*2* indicating a comparable number of patients with COPD in both groups. Nonetheless, a significantly higher incidence of postoperative air leaks was recorded in the 3D-CTBA-ID group compared to the 3DP-NIF group (33.3% *vs.* 7.6%, P<0.001). This observation, coupled with data on the precise representation of lung segments, suggested that sub-optimal representation and imprecise cutting of intersegmental planes contributed to air leaks in the 3D-CTBA-ID group. Conversely, in the 3DP-NIF group, unclear observation of intersegmental planes in five cases was attributed to incomplete cutting of collateral arteries during surgery within target lung segments. While lung tissue inherently possesses a 3D structure, it is reduced to a two-dimensional plane using precise tailoring techniques such as platform or linear cutting anastomosis for accurate resection, and stretching the residual lung tissue post-resection prevents compression and occult air leakage (30). Contrary to findings in previous research (31), the use of fibrin glue combined with absorbable polyglycolic acid material (NEOVEIL) in the present study effectively lowered the incidence of postoperative air leakage by covering the stretched intersegmental lung planes.

The results of the current study demonstrated that the combination of 3DP and ICG fluorescence thoracoscopic technology in lung segmental surgery offered significant advantages over the use of 3D-CTBA combined with the modified ID method. The utilization of 3DP technology to create patient-specific lung anatomy models enabled accurate localization of tumor tissues, visual identification of the anatomical structures and variations of lung segments, and the planning of the surgical resection area preoperatively and provided real-time navigation during thoracoscopy (*Figures 2B-2G*,*3D*). Furthermore, this approach considerably enhanced the accuracy and safety of thoracoscopic lung segment surgery by allowing real-time identification of blood vessels within the target area. Additionally, the incorporation of ICG fluorescence thoracoscopic technology facilitated the clear and rapid visualization of planes between resected lung segments (*Figure 3B*), thereby preventing incorrect or missed resections, ensuring sufficient surgical margins, reducing postoperative complications, and diminishing operation and anesthesia durations. Ultimately, these advancements improved surgical success rates while promoting swift postoperative recovery for patients.

The present study introduced several innovations: (I) preoperative 3D-CTBA reconstruction and the creation of individualized anatomical models through 3DP, enabling precise preoperative planning for patients by analyzing bronchial and vascular structures of lung segments. (II) The pioneering application of ICG fluorescence technology in conjunction with a 3D printed model to identify intersegmental planes during thoracoscopic segmental resection, allowing rapid and clear visualization. The comparison of traditional 3D-CTBA with the modified ID technique, combined with 3DP and NIF technology, demonstrated the advantages and application value of the latter.

However, this study had certain limitations that cannot be overlooked. To begin, the sample size was impacted by the high cost of 3DP (approximately $680 per unit) and

the time-consuming production process at this stage of the study. Hence, an expansion of the sample size in future studies is warranted to validate the accuracy and reliability of the findings. Secondly, a long-term follow-up is essential to evaluate both clinical outcomes and survival quality when employing the combination of 3D printed models with NIF technology in VATS.

## Conclusions

The integration of 3D printed models with NIF technology is highly valuable for conducting precise lung segmentectomies. This combination serves as a reliable technical safeguard, ensuring the safe and efficient execution of thoracoscopic pulmonary segmentectomy, thus demonstrating eligibility for clinical application.

## Acknowledgments

The authors appreciate the academic support from the Thoracic Department, Fujian Medical University Union Hospital. The authors give thanks to Ningbo Wedge Medical Technology Co., Ltd. and Shenzhen Yidimu Intelligent Technology Co., Ltd. for providing technical support for the 3D-CTBA and 3D printing technology. In addition, we thank Dr. Johnny (from the Home for Researchers editorial team) for revising the English of this manuscript.

*Funding:* This work was supported by Fuzhou Health Technology Project (No. 2021-S-wq32) and Startup Fund for Scientific Research, Fujian Medical University (No. 2023QH2024).

## Footnote

*Reporting Checklist:* The authors have completed the STROBE reporting checklist. Available at https://jtd.amegroups.com/article/view/10.21037/jtd-24-489/rc

*Data Sharing Statement:* Available at https://jtd.amegroups.com/article/view/10.21037/jtd-24-489/dss

*Peer Review File:* Available at https://jtd.amegroups.com/article/view/10.21037/jtd-24-489/prf

*Conflicts of Interest:* All authors have completed the ICMJE uniform disclosure form (available at https://jtd.amegroups.com/article/view/10.21037/jtd-24-489/coif). The authors have no conflicts of interest to declare.

*Ethical Statement:* The authors are accountable for all aspects of the work in ensuring that questions related to the accuracy or integrity of any part of the work are appropriately investigated and resolved. The study was conducted in accordance with the Declaration of Helsinki (as revised in 2013). The study was approved by the Medical Ethics Committee of Fuzhou Pulmonary Hospital, Fuzhou, Fujian Province, China (approval No. 2024004-01) and informed consent was obtained from all individual participants.



## References

1. Sung H, Ferlay J, Siegel RL, et al. Global Cancer Statistics 2020: GLOBOCAN Estimates of Incidence and Mortality Worldwide for 36 Cancers in 185 Countries. CA Cancer J Clin 2021;71:209-49.
2. Kinoshita F, Takenaka T, Yamashita T, et al. Development of artificial intelligence prognostic model for surgically resected non-small cell lung cancer. Sci Rep 2023;13:15683.
3. Şahin E, Kara A, Elboğa U. Contribution of nonattenuation-corrected images on FDG-PET/CT in the assessment of solitary pulmonary nodules. Radiol Med 2016;121:944-9.
4. Fong KY, Chan YH, Chia CML, et al. Sublobar resection versus lobectomy for stage IA non-small-cell lung cancer≤2 cm: a systematic review and patient-level meta-analysis. Updates Surg 2023;75:2343-54.
5. Zhu S, Xu W, Li Z, et al. Branching patterns and variations of the bronchus and blood vessels in the superior segment of the right lower lobe: a three-dimensional computed tomographic bronchography and angiography study. J Thorac Dis 2023;15:6879-88.
6. Isaka T, Mitsuboshi S, Maeda H, et al. Anatomical analysis of the left upper lobe of lung on three-dimensional images

 

with focusing the branching pattern of the subsegmental veins. J Cardiothorac Surg 2020;15:273.
7. Qiu B, Ji Y, He H, et al. Three-dimensional reconstruction/personalized three-dimensional printed model for thoracoscopic anatomical partial-lobectomy in stage I lung cancer: a retrospective study. Transl Lung Cancer Res 2020;9:1235-46.
8. Wang J, Xu X, Wen W, et al. Modified method for distinguishing the intersegmental border for lung segmentectomy. Thorac Cancer 2018;9:330-3.
9. Motono N, Iwai S, Funasaki A, et al. Low-dose indocyanine green fluorescence-navigated segmentectomy: prospective analysis of 20 cases and review of previous reports. J Thorac Dis 2019;11:702-7.
10. Sun Y, Zhang Q, Wang Z, et al. Is the near-infrared fluorescence imaging with intravenous indocyanine green method for identifying the intersegmental plane concordant with the modified inflation-deflation method in lung segmentectomy? Thorac Cancer 2019;10:2013-21.
11. Sun Y, Zhang Q, Wang Z, et al. Feasibility investigation of near-infrared fluorescence imaging with intravenous indocyanine green method in uniport video-assisted thoracoscopic anatomical segmentectomy for identifying the intersegmental boundary line. Thorac Cancer 2021;12:1407-14.
12. Ettinger DS, Aisner DL, Wood DE, et al. NCCN Guidelines Insights: Non-Small Cell Lung Cancer, Version 5.2018. J Natl Compr Canc Netw 2018;16:807-21.
13. Huang RJ, Chen SX, Han ZZ. 3D printed model combined with indocyanine green fluorescence thoracoscopic single-port segmental lung resection in early stage lung cancer. Chinese Journal of Experimental Surgery 2023;40:1850-4.
14. Ohtaki Y, Shimizu K. Anatomical thoracoscopic segmentectomy for lung cancer. Gen Thorac Cardiovasc Surg 2014;62:586-93.
15. Paul S, Altorki NK, Sheng S, et al. Thoracoscopic lobectomy is associated with lower morbidity than open lobectomy: a propensity-matched analysis from the STS database. J Thorac Cardiovasc Surg 2010;139:366-78.
16. Winckelmans T, Decaluwé H, De Leyn P, et al. Segmentectomy or lobectomy for early-stage non-small-cell lung cancer: a systematic review and meta-analysis. Eur J Cardiothorac Surg 2020;57:1051-60.
17. Wang X, Guo H, Hu Q, et al. Pulmonary function after segmentectomy versus lobectomy in patients with early-stage non-small-cell lung cancer: a meta-analysis. J Int Med Res 2021;49:3000605211044204.
18. Saji H, Okada M, Tsuboi M, et al. Segmentectomy versus lobectomy in small-sized peripheral non-small-cell lung cancer (JCOG0802/WJOG4607L): a multicentre, open-label, phase 3, randomised, controlled, non-inferiority trial. Lancet 2022;399:1607-17.
19. Zhang H, Li Y, Yimin N, et al. CT-guided hook-wire localization of malignant pulmonary nodules for video assisted thoracoscopic surgery. J Cardiothorac Surg 2020;15:307.
20. Wu Z, Zhang L, Zhao XT, et al. Localization of subcentimeter pulmonary nodules using an indocyanine green near-infrared imaging system during uniportal video-assisted thoracoscopic surgery. J Cardiothorac Surg 2021;16:224.
21. Ji Y, Zhang T, Yang L, et al. The effectiveness of three-dimensional reconstruction in the localization of multiple nodules in lung specimens: a prospective cohort study. Transl Lung Cancer Res 2021;10:1474-83.
22. Fu R, Chai YF, Zhang JT, et al. Three-dimensional printed navigational template for localizing small pulmonary nodules: A case-controlled study. Thorac Cancer 2020;11:2690-7.
23. Shiina N, Kaga K, Hida Y, et al. Variations of pulmonary vein drainage critical for lung resection assessed by three-dimensional computed tomography angiography. Thorac Cancer 2018;9:584-8.
24. Meershoek AJA, Loonen TGJ, Maal TJJ, et al. Three Dimensional Printing as a Tool For Anatomical Training in Lung Surgery. Med Sci Educ 2023;33:873-8.
25. Oizumi H, Kato H, Endoh M, et al. Techniques to define segmental anatomy during segmentectomy. Ann Cardiothorac Surg 2014;3:170-5.
26. Liu Z, Yang R, Cao H. Near-infrared intraoperative imaging with indocyanine green is beneficial in video-assisted thoracoscopic segmentectomy for patients with chronic lung diseases: a retrospective single-center propensity-score matched analysis. J Cardiothorac Surg 2020;15:303.
27. Misaki N, Chang SS, Igai H, et al. New clinically applicable method for visualizing adjacent lung segments using an infrared thoracoscopy system. J Thorac Cardiovasc Surg 2010;140:752-6.
28. Peeters M, Jansen Y, Daemen JHT, et al. The use of intravenous indocyanine green in minimally invasive segmental lung resections: a systematic review. Transl Lung Cancer Res 2024;13:612-22.
29. Bronstein ME, Koo DC, Weigel TL. Management of

 

air leaks post-surgical lung resection. Ann Transl Med 2019;7:361.
30. Zheng B, Xu G, Fu X, et al. Management of the inter-segmental plane using the "Combined Dimensional Reduction Method" is safe and viable in uniport video-assisted thoracoscopic pulmonary segmentectomy. Transl Lung Cancer Res 2019;8:658-66.
31. Nomori H, Abe M, Sugimura H, et al. Triple-layer sealing with absorptive mesh and fibrin glue is effective in preventing air leakage after segmentectomy: results from experiments and clinical study. Eur J Cardiothorac Surg 2014;45:910-3.

**Cite this article as:** Huang R, Du J, Xu G, Gong X, Qian J, Chen S, Zheng B, Chen C, Yang Z. Application of three-dimensional printed models with near-infrared fluorescence technology in video-assisted thoracoscopic surgery segmentectomy: a single-center propensity-score matching analysis. J Thorac Dis 2024;16(7):4474-4486. doi: 10.21037/jtd-24-489